

Design of a 480GHz Metamaterial Flat Lens

Cassandra N. Whitton¹, Jose V. Siles², Christopher E. Groppi¹, Philip D. Mauskopf¹, Adrian J. Tang²

The measuring of water vapor column densities and temperatures is relevant to many fields of study, including astrophysics, planetary science, and Earth science. For astrophysical and planetary science purposes in particular, such measurements are virtually impossible to perform without a space-based observatory due to the high attenuation introduced by water in the Earth's atmosphere. Observations of the 557 GHz line of ortho-water have been performed previously with large space-based instruments, but the ability to perform such observations with a cubesat would significantly increase the cost-effectiveness of such missions and thereby opens up previously unavailable science applications which would be financially impractical to perform with a larger platform.

For these reasons, we are designing a cubesat capable of spectroscopically resolving the 557 GHz and 1113 GHz lines of water vapor. Measurements performed with such a cubesat would allow us to gain information about the temperature, structure, and density of water vapor. Such a cubesat requires the miniaturization of several crucial technologies due to the small form factor and low weight requirements inherent in the cubesat standards. One such structure is the primary observing aperture. A metamaterial lens acting as the primary aperture is ideal for this purpose. Our metamaterial lens is a lens in which the focusing of light is achieved by using patterned elements of conductive material embedded in the lens structure as opposed to a traditional curved lens or Fresnel geometry. Such a lens can be made lightweight, flat, and can be designed to have near-zero reflections to reduce observing time.

As an intermediate step, we here present a design for a lightweight and flat metamaterial lens which operates at 480 GHz. The design has been simulated to measure its focusing ability as well as its reflectivity and attenuation at the necessary frequencies. Overall, we find very low reflective and optical losses at the design frequency (less than 5% each) and less than 20% conductive/dielectric loss.

Keywords—*terahertz, cubesat, metamaterial, lens, optics (key words)*

I. INTRODUCTION

Flat metamaterial optics may offer substantial improvements in the size, weight, and power (SWaP) of optics in space-based applications. This is of particular interest for Smallsat applications where SWaP restrictions are of paramount importance. The main characteristic of the proposed optics that results in dramatic improvements in SWaP resource requirements is the thin geometry of the metamaterial structure. In a traditional bulk lens, focusing is achieved through the transformation of a planar wavefront to a spherical wavefront with a dielectric of varying thickness. The required shape of the surface of the lens is governed by Snell's law to provide a focus at a given location. This shape results in a minimum required thickness of bulk dielectric. In

the sub-mm and THz, this thickness is at a minimum several mm and increases when a lens with a small f/D ratio is required. Zone plate lenses (e.g. a Fresnel lens) can help to address this problem, with a bandwidth penalty caused by the wavelength dependent design of the lens [3]. A gradient index lens would instead achieve this phase shift by altering the index of refraction of the lens over its surface, again creating a varying path-length over the lens. A mirror provides a similar transformation but through a reflective surface governed by the law of specular reflection. Again, this results in a material thickness of several mm at a minimum to create and support the reflective mirror geometry.

By contrast, a metamaterial flat lens can be less than a fraction of a mm thick, with a corresponding decrease in weight.

In addition, multi-layered metamaterial structures can effectively have anti-reflection coating built into them from their initial design. This can result in low reflective loss and thus significantly greater efficiency than a traditional curved lens. The lower thickness of such a flat lens can also result in significantly lower dielectric losses than an equivalent curved lens.

II. METHODS

Our design process is primarily based on the work of Pisano (Ref. [1]), with some key differences. Our overall design process is as follows:

- 1) Choose the primary optical characteristics of the lens: diameter, focal length, operating frequency.
- 2) Choose materials and secondary characteristics: dielectric substrate material, conductive material, thickness of dielectric and metal layers, and number of layers.
- 3) Subdivide the lens surface into pixels based on the operating frequency.
- 4) From the desired optical characteristics, determine the desired phase transformation that each pixel will apply as a function of frequency.
- 5) In HFSS (or equivalent EM simulation software), simulate varying sizes of individual conductive elements embedded in dielectric.
- 6) Using the results from HFSS, create a model which simulates the S-parameters of a single pixel, using transmission line theory.
- 7) In a scripting language, run an optimization script which tweaks the sizes of the conductive elements in order to find the best element sizes for each pixel in the lens.

For our design, we chose a diameter of 124mm, due to working with a manufacturing process which uses 150mm wafers with an exclusion zone around the edge. We chose a focal length of 150mm since we are interested in using these

¹ School of Earth and Space Exploration, Arizona State University, Tempe, AZ 85281 USA (email: cassandra.whitton@gmail.com) ² Jet Propulsion Laboratory, Pasadena, CA 91109 USA

lenses for cubesat applications where short focal lengths could be advantageous to save space. We chose an operating frequency of 480GHz in order to be able to test the lens with 500GHz VNA extenders that we have access to. In principle, our design process can be used to optimize across a bandwidth rather than a single frequency. We chose a single frequency for simplicity.

In step 2, we chose to use polyimide as our dielectric and aluminum as our conductive material, as well as a metal thickness of 0.5 μ m. Aluminum was chosen over copper because it can be dry-etched, which makes it easier to manufacture. We found the simulated difference in loss between copper and aluminum was less than 1%. The metal thickness was chosen to make the metal multiple skin-depths thick at our chosen frequency. We chose to use 10 metal layers (in between 11 polyimide layers). We chose a dielectric thickness of 10 μ m per polyimide layer. This ensures that the total lens thickness is roughly 110 μ m, which is approaching the maximum thickness that the manufacturing process can accept.

In step 3, we chose to subdivide our lens into square pixels with side dimension 120 μ m, or one fifth of a free-space 500GHz wavelength. This follows Pisano's recommendation.

In step 4, we differ from Pisano's process. While Pisano uses the Gaussian beam approximation to generate the phase pattern on the lens, we found that this approximation failed to accurately predict our lens focal length when we tested a 20GHz lens prototype [6]. We found the actual focal length was 10% longer than expected. Instead, we use the Gaussian beam approximation [3] to estimate the beam waist of a gaussian beam coupled to the lens from its focal point, based solely on the lens diameter and focal length. Then we use Fourier optics (as described in Ref. [2]) code written in matlab to simulate propagating the beam from the focal point to the lens surface. Then we use the simulated beam phase to give us the desired phase pattern for the lens.

In step 5, we simulated varying sizes of aluminum squares embedded within polyimide. Floquet ports were used to simulate a plane wave entering and then exiting the aluminum square, with periodic boundary conditions. Additional polyimide material (roughly a half wavelength) had to be added on both sides of the element and then de-embedded to ensure accurate results. Full S-parameters from 450-500GHz were simulated for roughly 100 different sizes of squares, ranging from 1% to 99% of a pixel length dimension.

In step 6, we model the S21 of each pixel. Note that each pixel is an alternating stack of 11 dielectric layers and 10 conductive elements. We combine the results simulated in step 5, and a model for the polyimide dielectric ($\epsilon_r = 3.5$ and $\tan\delta = 0.015$). This polyimide model is taken from THz measurements in Ref. [4] and verified by our own independent measurements of the material. To model a pixel, we convert the S-parameters of the thicknesses of polyimide layers and given sizes of conductive element to ABCD parameters, and then multiply them together, alternating polyimide-conductor-polyimide-conductor, etc. We take the characteristic impedance of the S-parameters to be the impedance of free space, since the lens inputs and outputs will be free space. A full explanation of this technique may be found in section 4.4 of Ref. [5].



Fig. 1. A zoomed-in image of a single layer of the lens manufacturing drawing. Each pink square will be a conductive element embedded in polyimide.

In step 7, we use the pixel model from step 6 in combination with the desired phase pattern found in step 4. The optimizer is given the freedom to alter the size parameter of each conductive element in the pixel. The goal function is created from the S21 of the pixel, as the product of the magnitude of S21 and the cosine of the phase difference between the desired and achieved S21. This ensures that both the transmittance and phase of the pixel are optimized for. Note that the optimization may be subject to additional constraints. In our case, the manufacturer's minimum feature size of 5 μ m limited the largest and smallest possible conductive element sizes that we could use.

Once each pixel in the lens has been optimized, we can convert each layer of the lens to a manufacturing file. One layer of the lens manufacturing drawing is depicted in Fig. 1.

We can also simulate the performance of the lens. In our case, we first use the S21 of the lens to see what a plane wave input to the lens would be transformed to in its output plane. We can then use the Fourier optics code described earlier to propagate that output wave to the lens's focal plane, then use this focal plane information to analyze the lens performance.

III. SIMULATION RESULTS

The results of simulating a plane wave propagated through the lens can be seen in Fig. 2. As a figure of merit, we use the Strehl ratio of the lens, which is defined as the peak intensity of the actual lens at its focal point divided by the peak intensity of an ideal lens of the same diameter at its focal point [7]. This helps to define the performance of the lens without requiring a specific feed source to couple to. A Strehl ratio of 1 is ideal.

We simulated the Strehl ratio of the lens at 480GHz to be 0.78. The Strehl ratio can be broken down into three inefficiencies: reflective loss, conductive/dielectric loss, and optical loss. We found the reflective efficiency to be 96.5%: that is, 3.5% of power incident on the lens is reflected. We found the dielectric/conductive efficiency to be 82%: that is, 18% of power that is not reflected from the lens is absorbed by the lens as heat. Finally, the optical efficiency of the lens

is 98.1%: 1.9% of the power that is output from the lens is scattered due to phase inaccuracy.

Performing these simulations over a wider frequency range, we find that the 3dB bandwidth (i.e. the bandwidth in which the Strehl ratio is at least half its maximum) is roughly 5%. The reflective and dielectric loss stay relatively constant while the optical loss drops quickly away from the center frequency.

IV. CONCLUSION

We have designed a flat lens that performs well at 480GHz. From our simulations, we can see that our lens has solid performance with a Strehl ratio of 0.78. The breakdown of inefficiencies demonstrate that, at least theoretically, our metamaterial's built-in anti-reflection coating is very effective, resulting in only 3.5% reflective loss. At the design frequency, optical efficiency is also very strong, leaving dielectric and conductive efficiency as the primary sources of loss.

It is possible, if additional performance is necessary, that the lens can be made thinner, or out of different dielectric material, to reduce the dielectric loss. Polyimide has a relatively high loss tangent of 0.015 at our design frequency, while some plastics such as high-density polyethylene or polypropylene have a loss tangent nearly an order of magnitude lower [3]. However, the plastics we can use are limited by the capabilities of our manufacturing partners.

The low frequency bandwidth of the lens is a downside, but not surprising given that the lens was optimized for a single frequency. Additional study will be done to see if we can increase the bandwidth by using wider optimizations without significantly decreasing the center-frequency performance. We are hopeful given successful experiments with this in, e.g., [1], where a roughly 30% fractional bandwidth is obtained.

We have recently received the first batch of manufactured lenses from our manufacturing partners and are currently working to characterize its performance with real measurements.

REFERENCES

- [1] Pisano, Giampaolo, et al., "Dielectrically Embedded Flat Mesh Lens for Millimeter Waves Applications", *Applied Optics*, Apr. 2013.
- [2] Davis, Kristina, et al., "Analysis Techniques for Complex Field Radiation Pattern Measurements", *Proceedings of SPIE*, 2018.
- [3] Goldsmith, Paul F., "Quasioptical Systems", 1998.
- [4] Sahin, Seckin, et al., "Dielectric Properties of Low-Loss Polymers for mmW and THz Applications", *International Journal of Infrared and Millimeter Waves*, Mar. 2019.
- [5] Pozar, David M., "Microwave Engineering: Fourth Edition", 2012.
- [6] Whitton, Cassandra N., et al. "Measurements and Simulations of a 20 GHz Metamaterial Lens", *31st IEEE International Symposium on Space Terahertz Technology*, Mar. 2020.
- [7] Strehl, Karl W. A. "Theory of the telescope due to the diffraction of light", 1894.

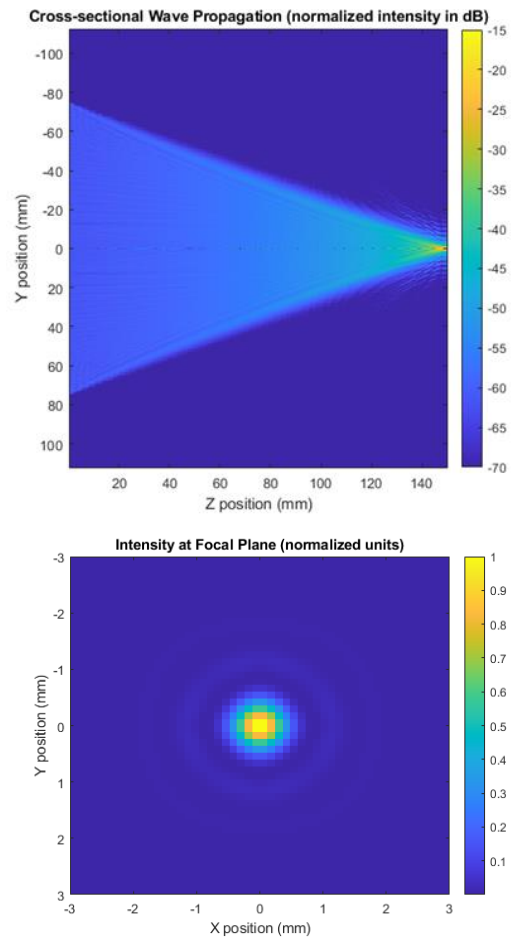


Fig. 2. Top: A cross-section of a Fourier-optics-simulated wave being propagated from the lens output (left) to the focal plane (right). Bottom: The intensity plotted at the lens focal plane, demonstrating an Airy pattern.